J Solid State Electrochem (2002) 6: 291–301
DOI 10.1007/s100080100240

ORIGINAL PAPER

P. Damlin · C. Kvarnström · A. Petr
P. Ek · L. Dunsch · A. Ivaska

In situ resonant Raman and ESR spectroelectrochemical study of electrochemically synthesized poly(*p*-phenylenevinylene)

Received: 29 May 2001 / Accepted: 10 July 2001 / Published online: 16 November 2001

Abstract The electrochemical synthesis of poly(*p*-phenylenevinylene) (PPV) and different modifications in the electronic distribution upon electrochemical p-doping (oxidation) and n-doping (reduction) of this polymer film have been studied in situ by resonance Raman spectroscopy, optical absorption spectroscopy and ESR spectroscopy. The polymer film has been prepared by electrochemical reduction of α,α,α′,α′-tetrabromo-*p*-xylene in dimethylformamide using tetraethylammonium tetrafluoroborate as the electrolyte salt. During electrochemical polymerization the position and relative intensities of the Raman bands change regularly as the chain length increases and finally converge on values reported for chemically prepared PPV. The Raman spectra for electrochemically polymerized PPV is compared to infrared-active vibration bands for electrochemically n-doped PPV. When the polymer undergoes redox reactions (doping-dedoping), shifts and broadening of Raman bands, compared to neutral PPV, are observed. Interpretation of the Raman spectra and the ESR results led to the conclusion that charge transfer in this system is mainly accomplished by polaron species formed upon doping of the polymer. In this reaction the quinoid structure is formed rather than the benzenoid structure.

Keywords Poly(*p*-phenylenevinylene) · Electrochemical polymerization · ESR spectroscopy · Raman spectroscopy

P. Damlin · C. Kvarnström (✉) · P. Ek · A. Ivaska
Process Chemistry Group,
c/o Laboratory of Analytical Chemistry,
Åbo Akademi University, 20500 Turku-Åbo, Finland
E-mail: ckvarnst@abo.fi
Fax: +358-2-2154479

A. Petr · L. Dunsch
Group of Electrochemistry and Conducting Polymers,
Institute of Solid State and Materials Research Dresden,
01107 Dresden, Germany

Introduction

For several years, conjugated polymers have been explored with the aim of providing new materials to modern technology, and to understand the physics emerging from these nonlinear semiconductors [1]. Poly(*p*-phenylenevinylene) (PPV) has become a very attractive polymer in this field because of its nonlinear optical properties [2], electroluminescence [3] and high electrical conductivity upon doping [4, 5, 6]. The electrical conductivity of PPV can be varied from an initially insulating to a highly conducting state by doping with electron donors (n-type doping) or acceptors (p-type doping). This doping reaction can be carried out chemically or electrochemically. The mechanism of electrical conduction in conducting polymers has been discussed in terms of self-localized excitations such as solitons, polarons and bipolarons, which are formed during the doping reaction. Conduction by polarons and bipolarons in particular is thought to be the dominant mechanism of charge transport in conducting polymers with nondegenerate ground state such as in PPV [1]. Polarons and bipolarons can be regarded as radical ions and divalent ions, respectively. Recently, a transverse 3D conduction model has been proposed for conducting polymers in which polarons interact with other polarons on neighbouring polymer chains and form diamagnetic polaron dimers [7, 8, 9]. The diamagnetic polaron dimer can be regarded as an alternative form of the diamagnetic bipolaron. These excitations that are charged with or without spin cause changes in the electronic distribution on the polymer backbone. They can be studied in conjugated polymers by using several techniques such as optical and magnetic spectroscopy, conductivity measurements, etc. Especially the resonance Raman scattering technique, which is one of the most sensitive techniques to study modifications in the electronic density, is a useful method in such structural studies.

In this work, PPV films were prepared by electrochemical reduction of α,α,α′,α′-tetrabromo-*p*-xylene.

Polymerization of the monomer (0.05 M) was done by potential cycling between 0 and –2.3 V in a solution containing 0.1 M tetraethylammonium tetrafluoroborate in dimethylformamide [10]. The film formation and intrachain modifications involving both polymeric structures and electronic distribution upon electrochemical n- and p-doping were studied in situ by resonant Raman, UV-Vis and ESR spectroscopy. The Raman spectra for the neutral form of PPV were compared with the IRAV spectra obtained by electrochemical n-doping of a PPV film.

Experimental

Chemicals

The monomer α,α,α′,α′-tetrabromo-*p*-xylene (**1**, Tokyo Kasei) was used as received. Tetraethylammonium tetrafluoroborate (TEA-BF_4, Acros Organics), tetraethylammmonium *p*-toluenesulfonate (TEATOS, Aldrich) and sodium perchlorate (Aldrich) were used as the electrolyte salts. $TEABF_4$ and TEATOS were dried at 80 °C and $NaClO_4$ at room temperature for 1 h under vacuum conditions before use. Acetonitrile (ACN, Lab-Scan) and dimethylformamide (DMF, Aldrich) were used as solvents. ACN was distilled over calcium hydride. ACN and DMF were purified by drying over activated aluminium oxide (Aldrich) before use.

Instrumentation

Resonance Raman experiments were performed with a Renishaw Raman microscope system equipped with a thermoelectrically cooled charged-couple device (CCD) detector. The excitation wavelength for the Raman scattering was provided by a diode laser operating in the near-IR range ($\lambda_L = 780$ nm) at low laser power (≤17 mW). The scattering signal was obtained at 90° configuration as shown in Fig. 1a. The spectroelectrochemical measurements were carried out in a three-electrode homemade flow-through electrochemical cell, permitting the in situ study of the chemistry at the electrode surface using Raman spectroscopy (Fig. 1a and b). The cell body was made of glass, the front window material was of quartz and the o-rings preventing leakage of the electrolyte were of Kalrez. A platinum disk (0.77 cm^2) was used as the working electrode and a platinum wire around it served as the counter electrode. The working electrode was polished with 0.3 and 0.05 μm Al_2O_3 before measurements. A silver wire coated with silver bromide was used as a pseudo reference electrode (+0.37 V vs. SCE calibrated

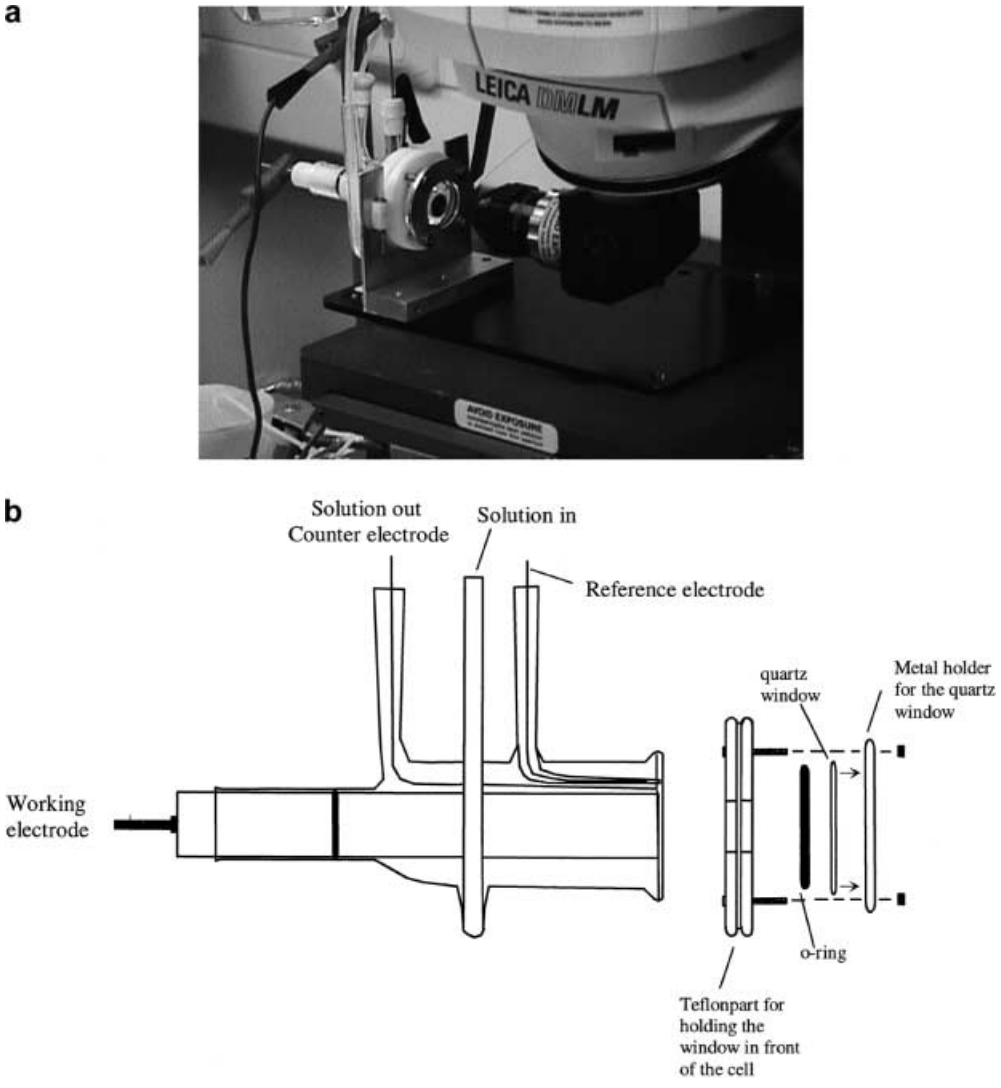

Fig. 1 The spectroelectrochemical cell used for the in situ Raman measurements: **a** side view of the cell; **b** scheme of the cell

vs. ferrocene in 0.1 M $TEABF_4$-DMF and +0.39 V when using ACN as the solvent). The silver wire was placed inside a glass capillary tubing the end of which was close to the working electrode (Luggin capillary design). All potentials are referred to this reference electrode unless differently stated.

Optical absorption measurements were carried out with a single-beam UV-Vis spectrophotometer (HP 8453) in the wavelength range 200–1200 nm using a photodiode array detector (PAR M 1461). A quartz cuvette with a three-electrode system was used in the UV-Vis measurements. The working electrode consisted of a platinum mesh (Goodfellow) of size 7 mm×18 mm. The platinum mesh was made from a wire of 0.06 mm diameter and had 1024 meshes per cm^2. A platinum wire was used as the counter electrode and a silver wire coated with silver bromide was used as the pseudo reference electrode. The polymer films were polymerized electrochemically at the surface of the platinum disk electrode when studied by Raman spectroscopy and on the platinum mesh in the UV-Vis measurements. A potentiostat (model 366A, EG&EG PAR) was used in the polymerization experiments.

In the ESR spectroscopic measurements an X-band spectrometer (ESP 300E, Bruker) was used. The electrochemical flat cell used in the electrochemical ESR investigations has been described earlier [11]. The platinum mesh used as the working electrode in the ESR measurements was the same as in the optical measurements but of dimension 5 mm×4 mm. An AgCl-coated wire within a capillary was used as the reference electrode (+0.37 V vs. SCE vs. ferrocene in 0.1 M $TEABF_4$-DMF). To avoid oscillations of the cell voltage in the ESR measurements, two counter electrodes were used. The Pd sheet counter electrode was placed below and the Pt wire counter electrode was situated above the flat part of the ESR cell. The electrochemical measurements were carried out in the flat cell by using a PC-controlled potentiostat PG 285 (HEKA Electronic, Lambrecht). The potential was provided by a digital-analog card which was also the triggering source for the ESR spectrometer.

Procedure

When the polymerization process of PPV was studied with the in situ Raman technique, different potential values between 0 V and –2.3 V vs. Ag/AgBr were applied to the working electrode. Raman spectra were recorded simultaneously at these potentials and the growth of the film could therefore be studied as function of the polymerization potential. In studying the electrochemical polymerization process of PPV, the Raman spectra are related to a reference spectrum taken at the bare Pt electrode at 0 V. The spectra reported are therefore difference spectra. After deposition of PPV at the surface of the platinum disc electrode the cell was flushed with monomer-free electrolyte solution in order to study the redox behaviour of the film. In the charging-discharging experiments, different potentials in the range 0 V to –2.1 V (n-doping) or between 0 V to 1.25 V (p-doping) were applied to the working electrode. When $NaClO_4$ was used as supporting electrolyte, the positive potential limit was kept at 1.15 V, which is safely below the degradation of that electrolyte. After each doping reaction the potential of the electrode was kept at 0 V for few minutes and the Raman spectrum of the neutral film was then recorded.

In the UV-Vis measurements, PPV was polymerized electrochemically onto the platinum mesh electrode by scanning the electrode potential 23 times between 0 V and –2.3 V vs. Ag/AgBr. The scan rate was 30 mV/s and the absorbance spectra were recorded at the end of each potential cycle.

For ESR measurements, PPV films were polymerized electrochemically on a platinum mesh electrode in a conventional three-electrode cell by potential cycling between 0 V and –2.3 V vs. Ag/AgBr (7 scans). The scan rate was 50 mV/s. After polymerization the film was thoroughly rinsed with DMF and was then placed inside the ESR flat cell filled with monomer-free electrolyte solution. Changes in the ESR signal were then studied during the charging-discharging reaction of the PPV film. During these reactions, 21 ESR spectra were recorded while the potential was scanned in the range –0.4 V to –2.1 V (n-doping) or 0 V to +1.4 V (p-doping). The scan rate was 10 mV/s.

In all polymerization experiments the concentration of the monomer material **1** was 0.05 M in a 0.1 M $TEABF_4$-DMF solution. In the charging-discharging experiments, 0.1 M electrolyte solutions of $TEABF_4$, TEATOS or $NaClO_4$ in DMF or ACN were used. In all experiments, oxygen was removed from the solutions by purging with dry nitrogen several minutes before the measurements.

Results and discussion

Electrochemical polymerization of PPV

In situ Raman spectroscopy

Potentiostatic polymerization of monomer **1** was studied by taking Raman spectra in situ during different stages of the polymerization process. Figure 2a shows the

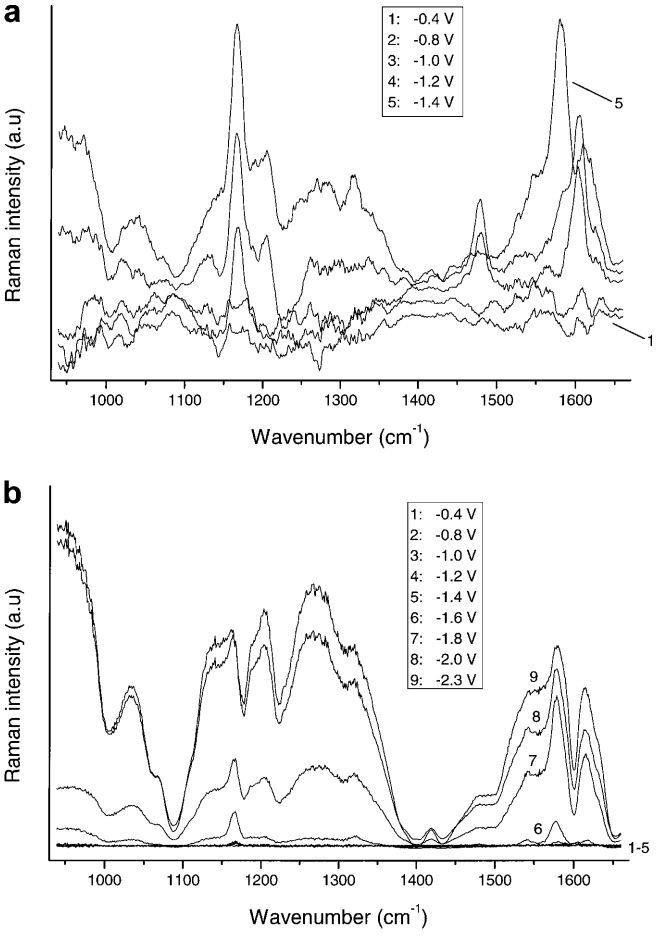

Fig. 2 **a** Changes in the Raman spectra ($\lambda_L = 780$ nm) obtained at the beginning of the polymerization reaction of α,α,α′,α′-tetrabromo-*p*-xylene. The polymerization was performed by applying potentials between –0.4 V and –1.4 V onto the working electrode in a 0.05 M solution of the monomer in 0.1 M $TEABF_4$-DMF. The inserted potential values indicate where each spectrum was recorded. **b** Changes in the Raman spectra obtained when extending the polymerization potential to –1.6 V, –1.8 V, –2.0 V and –2.3 V. Otherwise the conditions are the same as in **a**

Raman spectra obtained during the initial part of the polymerization process, when potentials between –0.4 V and –1.4 V were applied onto the working electrode.

Changes in the spectra in Fig. 2a can already be seen after –1.0 V was applied to the electrode. Most distinct changes take place at 1605 and 1176 cm^{-1}. When the polymerization potential was further increased to –1.4 V, a shift of these peaks to 1583 and 1171 cm^{-1} takes place. In addition, shoulders on the sides of these two main peaks at 1609, 1551 and 1204 cm^{-1} can be observed. In Fig. 2b the Raman spectra from Fig. 2a are shown together with the spectra obtained during further polymerization of PPV at the potential values of –1.6, –1.8, –2.0 and –2.3 V. Note the upscaling in Fig. 2a. It can be observed in Fig. 2b that when the polymerization potential was further increased to –1.6 V the positions of the bands forming the triplet near 1600 cm^{-1} are seen at 1546, 1582 and 1623 cm^{-1}. These values coincide with the bands obtained for the chemically polymerized PPV. According to previous results obtained for PPV and its oligomers [12, 13, 14], the bands at 1546 and 1582 cm^{-1} can be attributed to the phenyl ring (stretching of C=C and C-C, respectively) and the band at 1623 cm^{-1} to the vinyl group (stretching of C=C). The band at 1171 cm^{-1} can be assigned to mixtures of C-C stretching and C-H bending of the phenyl ring [15]. A downshift in the wavenumbers of the bands in the triplet near 1600 cm^{-1} has also been obtained for chemically synthesized PPV and its oligomers when the conjugation length increases [14, 16, 17, 18, 19]. The following downshifts has been observed when going from the shortest oligomer to the polymer: 1607 and 1566 cm^{-1} for 4,4′-dimethyl-*trans*-stilbene, 1593 and 1554 cm^{-1} in 1,4-bis(4-methylstyryl)benzene, 1589 and 1552 cm^{-1} in 4,4′-bis(4-methylstyryl)-*trans*-stilbene and, finally, 1582 and 1547 cm^{-1} in PPV [14]. Small variations in the band position have been reported also for the group of bands around 1170 cm^{-1} when the chain length of the PPV oligomers is increased [18]. A further proof for the increase in the conjugation length with the polymerization potential, in addition to the downshift observed in the 1650–1530 cm^{-1} range, can be found when looking at the ratio of the intensity of the bands at 1546–1571 cm^{-1} and 1625–1638 cm^{-1}. This ratio should increase with the number of repeating units [20, 21], which was also observed in the Raman spectra in Fig. 2a. From the results shown in Fig. 2a and b it can be concluded that, during electrochemical polymerization of PPV, short-chain oligomers are formed in the potential range –1.0 to –1.4 V. When the potential is increased to –1.6 V and beyond, the wavenumber and intensity of the bands in the Raman spectra converge on the same values that are observed in chemically polymerized PPV. Similar observations have also been found when studying electrochemical polymerization of PPV with the electrochemical quartz crystal microbalance (EQCM) and Fourier transform infrared (FTIR) spectroscopy [22, 23]. In those studies a mass increase and the appearance of IR bands reported for PPV was observed first after the potential had reached –1.6 V during the first scan in the potentiodynamic polymerization of PPV. A further increase in the intensity of the bands of PPV with increasing polymerization potential can also be seen in Fig. 2b. This increase is due to further coupling of oligomer segments. The negative peaks at 1007, 1063, 1088, 1307, 1401 and 1434 cm^{-1} originate from the solvent DMF [24]. The decrease in the intensity of solvent peaks is due to growth of the PPV film at the electrode surface and subsequent decrease of DMF concentration at the surface of the electrode. The baseline distortion in the spectra 7–9 in Fig. 2b originates from lack of compensation of the strong solvent peaks in the reference spectrum.

In situ UV-Vis spectroscopy

The optical absorption spectra obtained upon polymerization of compound **1** by potential cycling between 0 V and –2.3 V are shown in Fig. 3. The UV-Vis spectra

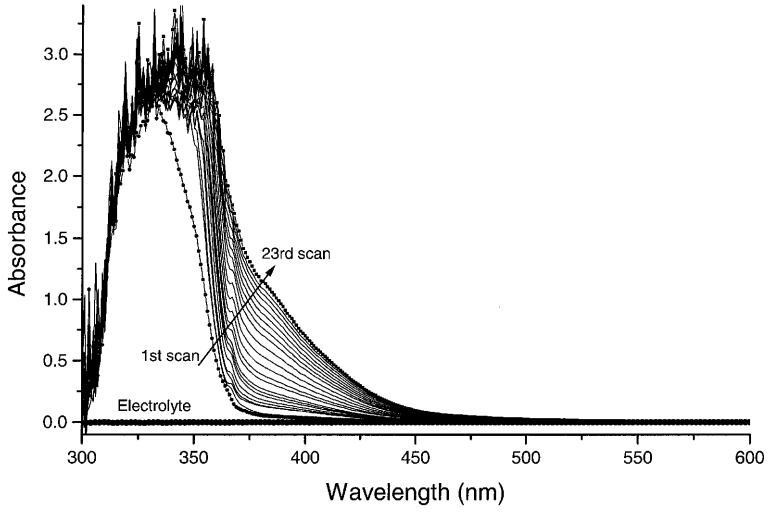

Fig. 3 In situ UV-Vis absorption spectra recorded during the electrochemical polymerization of α,α,α′,α′-tetrabrormo-*p*-xylene. The potential cycling was performed between 0 V and –2.3 V (23 scans) in a 0.05 M solution of monomer in 0.1 M $TEABF_4$-DMF. The absorption spectra were recorded at the end of each scan at –2.3 V. The *dotted* and the *squared lines* indicate the spectra taken at the end of the 1st and 23rd polymerization cycles, respectively. The *bold line* shows the response from monomer-free electrolyte solution in the potential range 0 V to –2.3 V

are recorded at the end of each sweep to the negative direction, i.e. at –2.3 V. For every cycle an increase in the absorbance in the range 370–470 nm can be observed, indicating the growth of the oligomer material on the electrode. The broad absorbance peak in the range 300–360 nm is due to intermediate products formed in the electrochemical polymerization reaction. These intermediates will be discussed in a separate paper. The thick line at zero absorbance shows the UV-Vis spectrum of the pure electrolyte in the same potential range as used in the electrochemical polymerization reaction.

Considering the onset of the $\pi \rightarrow \pi^*$ electron transition reported in the literature for different oligomers of PPV [18, 25], we may conclude that the effective conjugation length of electrochemically polymerized PPV in our experiments is in the order of five units compared to about eight units for standard PPV. On the other hand, the Raman spectra shown in Fig. 2b indicate an increase in the conjugation length with the applied polymerization potential until the values reported for the Raman bands of PPV are finally reached. The blue shift of the absorbance peak in Fig. 3 for electropolymerized PPV compared to the value between 460 and 500 nm reported for a dry chemically polymerized PPV film could be due to more conformational twisting of the molecules in the solution than in the solid phase. This kind of red shift in the UV-Vis spectra in going from the solution to the solid phase has been reported for PPV and its oligomers [26].

Electrochemical n- and p-doping of PPV

In situ resonant Raman spectroscopy

Resonance effects in conjugated polymers are usually seen as a strengthening of the Raman modes originating from the parts in the polymer that also gives rise to an optical absorption close in energy of the excitation line. Optical absorption maxima in the Vis-NIR region have been reported to be at 640 and 1340 nm for electrochemically doped PPV (chemically synthesized) [27, 28]. Electrochemically polymerized PPV (at –2.1 V, n-doped) gives absorption maxima around 700 and 1240 nm. Resonance Raman spectra in this work have been recorded using the excitation line in the NIR ($\lambda_L = 780$ nm). This line matches the energy of the electronic transitions of doped segments. The PPV films are electrochemically doped, which enables the study of changes in the electronic structure of the polymer in a controlled and reversible way. The changes in the Raman spectra upon n-doping and p-doping in different electrolyte media will be studied in the following section.

Figure 4 shows the Raman spectra recorded during potential scanning of PPV in 0.1 M TEATOS-DMF solution in the range 0 V to –2.1 V. In this potential range, *n-doping* of PPV takes place. The inset in Fig. 4 shows the cyclic voltammogram of a PPV film in the same electrolyte in the potential range –0.3 V to –2.1 V. At a low doping level the Raman spectrum of PPV is practically unchanged in comparison to the pristine

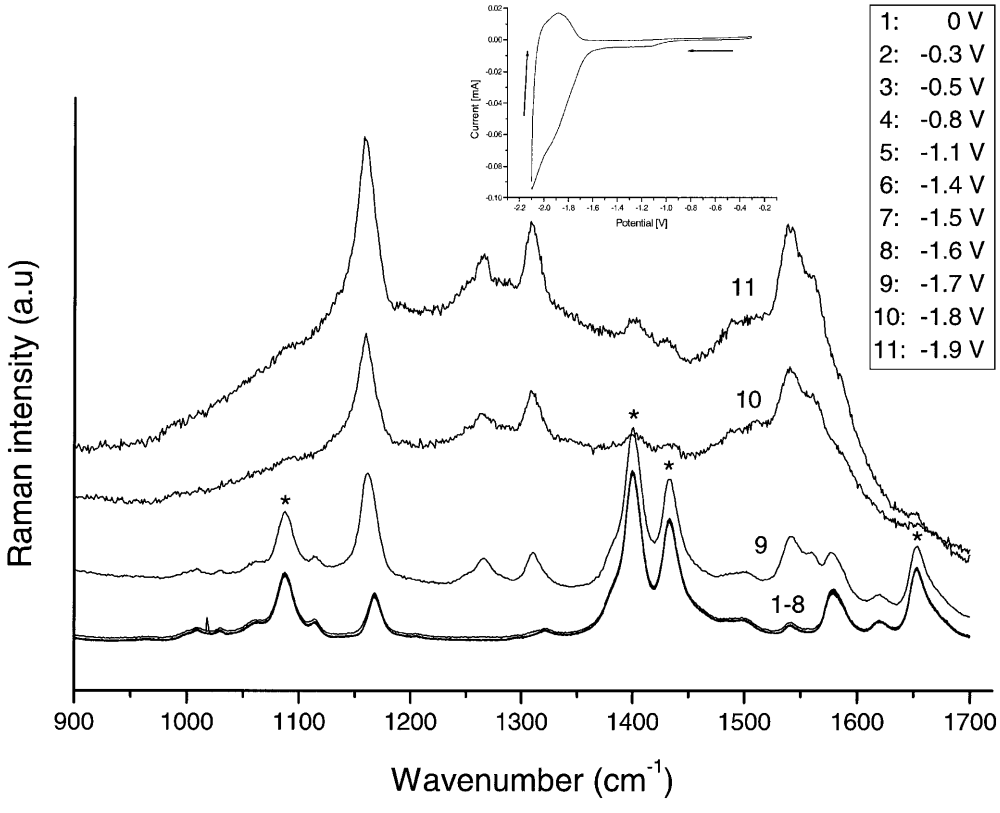

Fig. 4 In situ Raman spectra ($\lambda_L = 780$ nm) recorded during the n-doping reaction of an electrochemically polymerized PPV film in 0.1 M TEATOS-DMF. The inserted potential values are the potentials where each spectrum was recorded. The peaks marked with an *asterisk* (*) are due to the solvent DMF. The *insert* shows the cyclic voltammogram of PPV in 0.1 M TEATOS-DMF solution taken in the potential range –0.3 V to –2.1 V. The film was polymerized in a 0.05 M monomer solution with 0.1 M $TEABF_4$-DMF by potential cycling between 0 V and –2.3 V (7 scans)

polymer. The main spectral changes arise in the 1500–1700 cm^{-1} region upon further n-doping (–1.7 V). The gradual transformation of neutral polymeric sequences into the n-doped form is especially evidenced by the vanishing of the Raman band at 1625 cm^{-1}, assigned to the stretching mode of the C=C bond of the vinyl group in neutral PPV [21]. The bands that are seen in Fig. 4 upon n-doping of the PPV film are listed in Table 1. Raman bands due to the solvent DMF can clearly be identified. They are marked with an asterisk (*) in Fig. 4. These bands do not coincide with the bands of the polymer, except in the range 1400–1450 cm^{-1}. After the n-doping potential cycle the film was held at 0 V for several minutes, during which process the film was converted to undoped form. The Raman spectrum of this film was similar to the spectrum of the neutral form of PPV. The Raman spectra obtained during the second cycle were identical with the spectra from the first cycle. It should be mentioned that the same reversibility was observed in every charging-discharging reaction studied in this work.

When 0.1 M $TEABF_4$-DMF was used as the electrolyte during the n-doping reaction of PPV, the same bands as in Fig. 4 were observed in the Raman spectra. The only difference was the potential at which changes in the Raman spectra started to appear. In this case it was –1.8 V compared to –1.7 V when TEATOS was used as the electrolyte salt. The electrochemical switching between the doped and undoped states involves both electron and ion transport within the film. Different factors can influence the rate of counter ion transport through the redox active layer. Generally it has been stated that the degree of solvent swelling, size of supporting electrolyte ions and morphology of the film are some of the most important factors that influence the charging and discharging mechanism of the polymer layer [29]. Expected similarities in the Raman spectra obtained with different electrolytes are due to the fact that Raman spectroscopy measures the doping-induced perturbations on the intrachain scale, independently from the counter ion responsible for the charge transfer. Minor influences on the Raman mode are assumed to originate from the Coulombic attraction between the charged soliton and dopant ion.

The influence of the solvent on the n-doping reaction was studied by changing the solvent from DMF to ACN. The spectra obtained during electrochemical n-doping of PPV in 0.1 M $TEABF_4$-ACN solution are shown in Fig. 5. The cyclic voltammogram of a PPV film in this electrolyte is rather similar to the one shown as inset in Fig. 4. The bands that appear upon n-doping of PPV in 0.1 M $TEABF_4$-ACN are also listed in Table 1.

When comparing the spectra in Figs. 4 and 5, no distinct differences in the wavenumber of the bands can be observed. Compared to DMF, the only strong Raman band from ACN is located at 1369 cm^{-1}, which enables the study of the doping-induced changes in the wavenumber range 1400–1450 cm^{-1}. As can be seen in Table 1, the Raman bands obtained by electrochemical n-doping of PPV are rather similar to those reported in the literature for intermediate sodium-doped PPV [21]. Some of the bands given in Table 1 are rather weak, but still observable. Orion et al. [21] were able to interpret these weak bands as doping-induced bands by using different excitation wavelengths. Sakamoto et al. [30] have reported the appearance of the band at 1560 cm^{-1} as an indication of intermediate doping. This band can be found in all of our spectra taken during electrochemical n-doping. In sodium-doped PPV this band could not be seen at high doping levels, owing to the strong intensity of the bands at 1537 and 1578 cm^{-1} [21].

The spectral changes taking place during *p-doping* of PPV in 0.1 M $NaClO_4$-ACN are shown in Fig. 6. The inset in Fig. 6 shows the cyclic voltammogram of a PPV film in the potential range 0–1.15 V in 0.1 M $NaClO_4$-ACN solution. Similarly, as in the case of n-doping, the main changes can be seen in the wavenumber range

Table 1 Raman frequencies (in cm^{-1}) observed for neutral and electrochemically n-doped PPV at –1.9 V (column 2) and –2.0 V (column 3) ($\lambda_L = 780$ nm) as well as the values for intermediate sodium vapour doped PPV ($\lambda_L = 676.4$ nm) [21]. The bands that are weak in intensity are marked with (w)

Neutral PPV	n-doping		
	0.1 M TEATOS-DMF	0.1 M $TEABF_4$-ACN	Sodium vapour [21]
1623	–	–	–
1582	1580	1578	1578
–	1560	1561	1560
–	1539	1540	1537
1546	1509	1513	1509
–	1468 (w)	1470 (w)	1465 (w)
1408	–	1414	1414
–	1340 (w)	1340 (w)	1340 (w)
1322	1310	1310	1312
1300 (shoulder)	1288 (w)	1288 (w)	1290 (w)
–	1266	1266	1265
–	1243 (w)	1244 (w)	1245 (w)
–	–	–	1215
1171	1172	1172	1172
–	1158	1159	1155
966	–	–	–

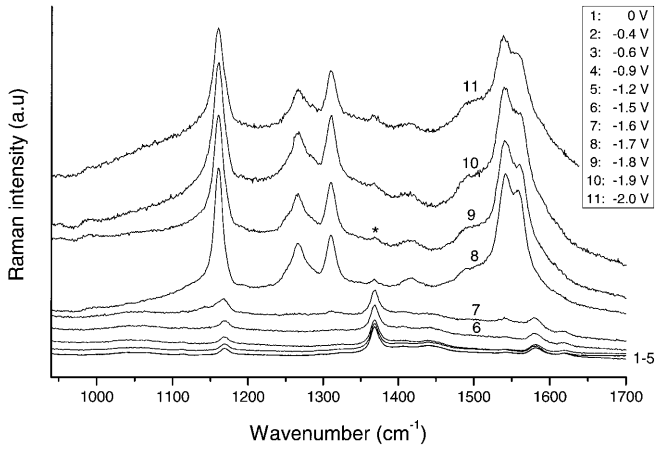

Fig. 5 In situ Raman spectra ($\lambda_L = 780$ nm) of n-doping of PPV recorded in 0.1 M $TEABF_4$-ACN. The inserted potential values are the potentials where each spectrum was recorded. The solvent peaks are indicated with an *asterisk* (*). The same conditions as given in Fig. 4 were used in the polymerization process

1500–1700 cm^{-1}. Also in p-doping a regular decrease of the band at 1625 cm^{-1} is observed (stretching of the vinylene C=C bond), indicating that structural modifications of the polymer chain takes place upon the p-doping reaction.

The intensive band observed at 1564 cm^{-1} and the shoulder at 1515 cm^{-1} correspond to the ring C-C stretching vibration of doped segments. The corresponding bands in neutral PPV are found at 1582 and 1546 cm^{-1}, respectively. Downshifts of these bands have been attributed to the distortion of the polymer chain, leading partially to a quinoid structure [13]. The Raman bands that appear in Fig. 6 upon p-doping of electrochemically polymerized PPV, together with reported values of bands in p-doped chemically polymerized PPV [28, 31], are listed in Table 2. When PPV was p-doped in $TEABF_4$-ACN, identical spectra with those shown in Fig. 6 were obtained. The only difference was the potential at which changes in the Raman spectra started to appear (at +1.0 V in $TEABF_4$-ACN).

Spectra obtained during n- and p-doping of PPV show doping-induced broadening and shifts of some bands compared with neutral PPV. All peaks grow strongly in intensity upon doping. Attempts to explain the doping-induced changes in the Raman spectra for PPV by calculations based on a valence-force model [13, 32, 33] have been reported, as well as a study of the doping-induced bands obtained for low molecular weight model compounds of PPV [27, 30, 34, 35]. Among the numerous force constants used in these calculations, a important role is played by those which characterize the C-C bonds in the benzene rings (F_{t^2} and $F_{t'^2}$) and in the vinyl group (F_{R^2} and F_{D^2}). The structural description of the force constants as described in the literature are shown in Scheme 1 [13].

The calculations have shown that upon doping the values for the force constants F_{R^2} and $F_{t'^2}$ decrease whereas F_{D^2} and F_{t^2} increase. These variations in the C-C stretching modes describe the quinoid structure, which is

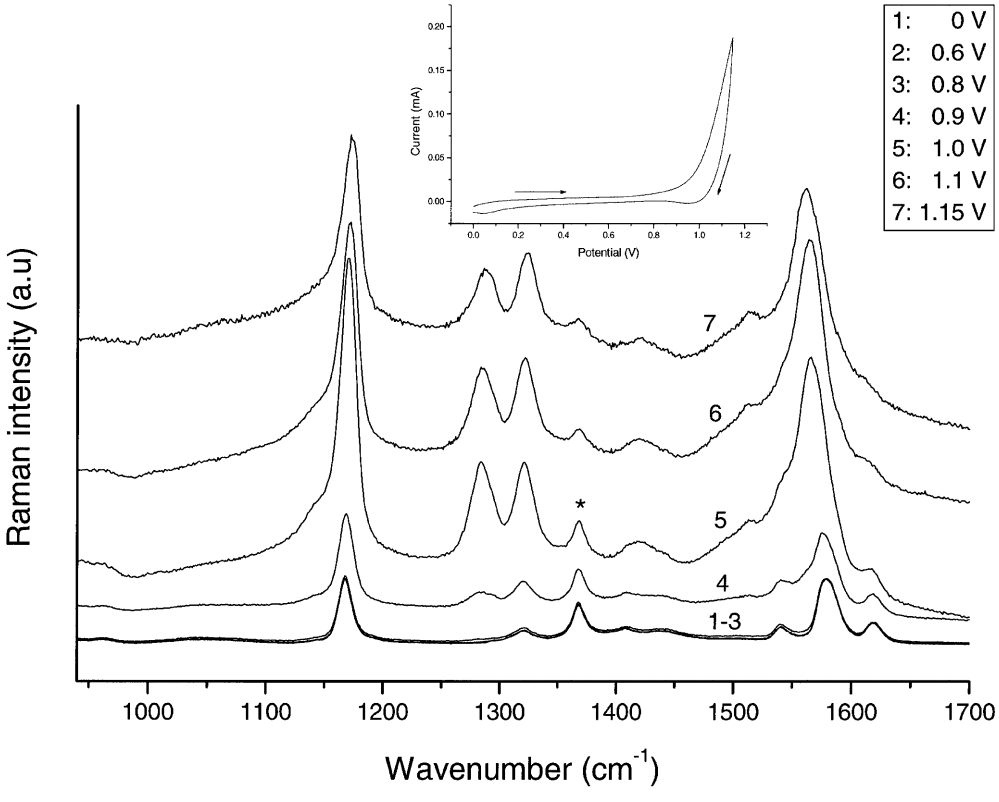

Fig. 6 In situ Raman spectra ($\lambda_L = 780$ nm) recorded during the p-doping of an electrochemically polymerized PPV film in 0.1 M $NaClO_4$-ACN. The inserted potential values are the potentials where each spectrum was recorded. The peak marked with * is due to the solvent ACN. The *insert* shows the cyclic voltammogram of PPV in 0.1 M $NaClO_4$-ACN solution taken in the same potential range. The polymerization conditions were the same as in Fig. 4

Table 2 Raman frequencies (in cm^{-1}) observed for neutral and electrochemically p-doped PPV at 1.25 V (column 2) and 1.15 V (column 3) using 780 nm as the excitation wavelength. The reported values for p-doped PPV at 1.3 V are given in column 4 ($\lambda_L = 676.4$ nm) [28]. The bands that are weak in intensity are marked with (w)

Neutral PPV	p-doping		
	0.1 M $TEABF_4$-ACN	0.1 M $NaClO_4$-ACN	0.2 M $TBABF_4$-ACN [28]
1623	1615 (w)	1610 (w)	1605 (w)
1582	1564	1564	1568
1546	1515	1514	1523
1408	1427	1422	1430
1322	1324	1322	1330
1300 (shoulder)	1286 (w)	1286 (w)	1296 (w)
–	–	–	1280
1171	1173	1172	1176
–	1143 (w)	1144 (w)	1147 (w)
966	–	–	–

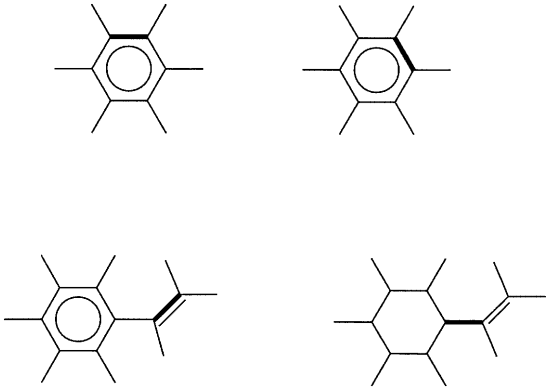

Scheme 1 Structural description of the force constants which characterize the C-C bonds of the benzene rings, F_{l^2} and $F_{l'^2}$, and the vinyl group, F_{D^2} and F_{R^2} respectively [13]

induced in PPV upon doping. Based on resonance Raman studies for radical ions and divalent ions derived from appropriate model compounds, it has been possible to attribute the observed changes in the Raman spectra of doped PPV to polarons and bipolarons [27, 30, 34, 35]. It was observed that the relative intensities of the new bands obtained upon doping depend on the excitation wavelength, but their positions, however, remain unchanged. The polaron bands were found to decrease when the excitation goes to the red range and further to the NIR range. The bipolaron bands, on the contrary, were found to be enhanced with red and IR excitations. The Raman spectra of n- and p-doped electrochemically polymerized PPV show coexistence of polaronic and bipolaronic species, which were also observed in doped chemically polymerized PPV [21, 28]. Polarons, however, were the main species in electrochemically polymerized PPV. Upon doping, the bands at 1171 and 1582 cm^{-1} (n-doping, Fig. 4) and at 1322 cm^{-1} (p-doping, Fig. 6) remain at about the same frequencies as in the neutral polymer, indicating stability of the aromatic ring against modifications in the electronic distribution. As a consequence, the force constants are maintained rather unchanged [21]. Upon doping the frequencies of some of the bands of neutral PPV shift due to structural modifications. In this case also an increase/decrease in the force constants is observed. In Tables 1 and 2 the wavenumbers of the Raman bands for neutral and doped PPV are listed parallel in order to show the shift of the bands upon doping.

The Raman spectra of neutral (a), p-doped (b), n-doped PPV (c) and the IR-active vibration bands for n-doped PPV (d) are shown in Fig. 7. The spectra were taken in 0.1 M $TEABF_4$-ACN solution at 0, +1.25 and –2.1 V. The Raman spectra show that the bands of neutral PPV are shifted in both doping processes. The results obtained with model compounds with different chain lengths have shown that the distribution of polarons and bipolarons in doped PPV is influenced by the type of doping (oxidation or reduction) [27]. Upon n-doping, a coexistence of polarons and bipolarons of various lengths was found. However, the resonance Raman spectra of p-doped model compounds showed that positive polarons and bipolarons extended over almost the same number of monomer units [27]. When the Raman spectra of n- and p-doped PPV in Fig. 7 were compared with the spectrum of neutral PPV, the changes observed were similar, as earlier reported for n- and p-doped chemically synthesized PPV [21, 28]. In the former paper [21] the excitation wavelength was $\lambda_L = 676.4$ nm and a low sodium concentration was used in the chemical n-doping reaction (intermediate doping level). The same excitation wavelength was also used in the latter paper [28] and p-doping was performed in a 0.1 M $TEABF_4$-ACN solution at +1.3 V. In Fig. 7 the differences between the spectra of n- and p-doped PPV are most evident in the wavenumber range 1500–1650 cm^{-1}. In this range the Raman bands show larger shifts upon n- than p-doping compared with the bands of neutral PPV. The difference in shift can be due to variations in distribution of negative and positive charge carriers and the resulting structure of the neighbouring backbone environment.

The n-doping induced IR-active vibration (IRAV) spectra recorded at –2.1 V (d) is also shown in Fig. 7. The spectrum was recorded in 0.1 M $TEABF_4$-DMF solution in an experimental setup described earlier [23]. The vibrational spectra of conjugated conducting polymers have been analyzed in terms of the effective conjugation coordinate (ECC) theory [1, 36]. The effective conjugation coordinate, $\mathit{Я}$, describes the evolution of the

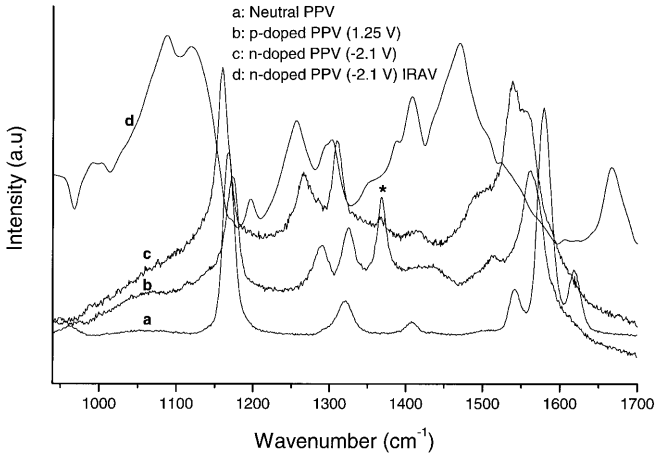

Fig. 7 Raman spectra ($\lambda_L = 780$ nm) of (*a*) neutral PPV, (*b*) p-doped PPV at +1.25 V, (*c*) n-doped PPV at –2.1 V and (*d*) the IRAV spectrum of n-doped PPV. All Raman spectra and the IRAV spectrum were recorded in situ in 0.1 M $TEABF_4$-ACN. The PPV film was polymerized electrochemically in a 0.05 M monomer solution with 0.1 M $TEABF_4$-DMF by potential cycling between 0 V and –2.3 V (7 scans)

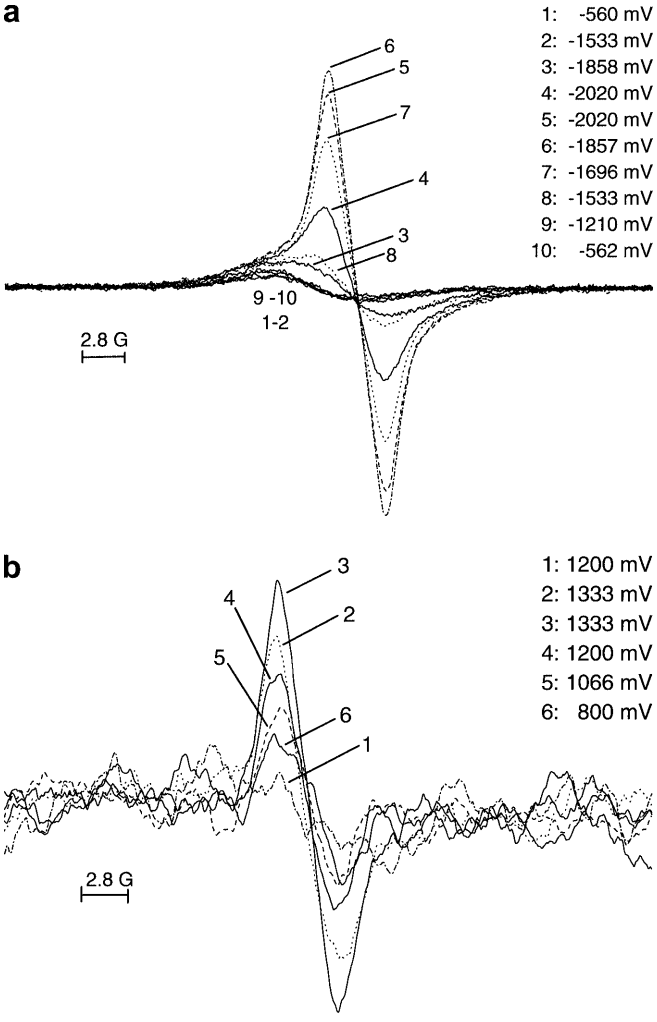

Fig. 8a, b In situ ESR signals obtained during doping and dedoping of a PPV film in 0.1 M $TEABF_4$-DMF. **a** n-doping by potential scanning between –0.4 V and –2.1 V. **b** p-doping by potential scanning between 0 V and 1.4 V. The scan rate used was 10 mV/s. The inserted potential values indicate where each ESR spectra was recorded. The PPV films were prepared electrochemically in a 0.05 M monomer solution with 0.1 M $TEABF_4$-DMF by potential cycling between 0 V and –2.3 V (7 scans)

structure of the polymer CC skeletal atoms in going from the ground (aromatic) state to the excited (quinoid) state. The originally IR-inactive Я mode of the neutral polymer film becomes strongly IR active due to lowering of the electrical symmetry caused by the polarization of the bonds upon inducing positive or negative charges. These IRAV bands correspond to the totally symmetric Raman active vibrational A_g modes. Once Я is defined it is possible to express the corresponding vibrational force constant, $f_Я$, a parameter used for the calculation of the vibrational frequencies. This force constant indicates the effective conjugation within the chain. When applying the ECC theory to PPV it has been shown that when the effective conjugation increases, $f_Я$ decreases and the frequencies of the bands shift toward lower values [36, 37]. Similar shifts as reported elsewhere [36, 37] can be observed in Fig. 7 when comparing the Raman spectra of neutral PPV with the IRAV spectra of n-doped PPV.

In situ ESR spectroscopy

Generally a bipolaron has been described to be more stable than two polarons in an idealized infinite polymer chain [38, 39]. Shimoi and Abe [40], on the other hand, demonstrated a higher stability of polarons than of bipolarons in the case of the intermediate strength of the Coulomb interaction by using the Pariser-Parr-Pople model combined with the Su-Schrieffer-Heeger model of electron-lattice coupling and a Brazovskii-Kinova-type symmetry-breaking interaction. Existence of chain endings and other conjugation breaks and transverse 3D interaction, either between adjacent chains or through the dopant [7, 8, 9], can also stabilize the polaron. The stability of polarons could explain the experimental observations made by resonance Raman spectroscopy reported in this article and by other research groups [21], where bands assigned to polarons can be seen independent of the doping level. With the ESR technique it is possible to investigate the mobile spins related to extrinsic doping-generated charge carriers. In Fig. 8a the change in the ESR signal upon n-doping and following dedoping of PPV in 0.1 M $TEABF_4$-DMF is shown.

As can be seen in Fig. 8a, the intensity of the ESR signal is low in the beginning of the scan and only after approximately –1.6 V does the amount of mobile spins increase. This coincides with the potential where an increase of the Faradaic current can be seen (inset in Fig. 4). During dedoping a decrease in the number of spins is observed, approaching the same level as in the beginning of the experiment. The higher ESR intensity

at the end of the cycle compared to the beginning of the n-doping cycle can be explained by a slow discharge of the electrochemically polymerized PPV film. For conducting polymers it is well known that at high doping levels the polaron concentration decreases due to recombination of polarons ($S=0$) to bipolarons ($S=1/2$). In ESR spectroscopy this is observed as a decrease in the number of spins. During the reduction reaction of the PPV film in Fig. 8a, no decrease in the number of spins at the highest doping level was observed. This, together with the Raman results of n-doped PPV in Fig. 4, suggests that only an intermediate level of doping is reached where the polarons still are the dominant species. The same kind of ESR result as in Fig. 8a was also obtained when ACN instead of DMF was used as the solvent. In Fig. 8b the change in the ESR signal upon p-doping of PPV in 0.1 M $TEABF_4$-ACN is shown. Compared to the n-doping experiments, the ESR signal is much weaker. Despite the low intensity of the signal, we still may draw the conclusion that polarons are created during p-doping of PPV and that the doping process is reversible.

Conclusions

In this paper the formation of PPV by electrochemical reduction of monomer **1** and the structural modifications induced by electrochemical p- and n-doping in different electrolyte solutions of the polymer film have been studied by in situ resonant Raman, optical absorption and ESR spectroscopy. The Raman spectra obtained during electrochemical polymerization of monomer **1** show a downshift of the bands in the triplet near 1600 cm^{-1} with the polymerization potential. These shifts indicate that the conjugation length increases with the polymerization potential. The bands reported for PPV are obtained when the polymerization potential of –1.6 V is reached. The IRAV bands of n-doped PPV were frequency downshifted when compared with the Raman spectra of neutral PPV. This is in good agreement with the calculations based on the effective conjugation coordinate theory. During electrochemical charging-discharging processes of the PPV film, shifts and broadening of existing bands together with a remarkable increase in intensity in the Raman spectra were observed compared with the spectrum of neutral PPV. The changes in the C-C stretching modes can be explained by the presence of the quinoid structure along the PPV chains. In the Raman spectra of doped (both n- and p-doped) PPV the positions of the bands show coexistence of polaronic and bipolaronic species, although the polaronic species are more dominant. This was further confirmed by the in situ ESR studies. Therefore the quinoid structure can be assigned to polaron species. The stability of these species can be explained by assuming an intermediate level of doping in the PPV films. The Raman spectra obtained were very similar in all the n-doping experiments, even when different electrolyte salts were used in the doping reaction. Similar results were also obtained in p-doping experiments. These results indicate that the Raman responses of PPV originate mainly from perturbations within the polymer chains. The shifts of the bands obtained upon doping compared with the bands of neutral PPV, however, were different and depended on the type of doping.

Acknowledgements The financial support from the Deutsche Akademische Austauschdienst and from the Academy of Finland, Process Chemistry Group (Finnish Centre of Excellence Programme 2000–2005) is gratefully acknowledged. The in situ UV-Vis measurements were performed at the Laboratory of Prof. J. Kankare at the University of Turku, who is gratefully acknowledged. P. Damlin is grateful for the support from Graduate School of Materials Research.

References

1. Skotheim TA, Elsenbaumer RL, Reynolds JR (1998) Handbook of conducting polymers, 2nd edn. Dekker, New York
2. Singh BP (1988) Polymer 29:1940
3. Burroughes JH, Bradley DDC, Brown AR, Marks RN, Mackay K, Friend RH, Burn PL, Holmes AB (1990) Nature 347:539
4. Shirakawa H, Louis EJ, MacDiarmid AG, Chiang CK, Heeger AJ (1997) Chem Commun 578
5. Chiang CK, Fincher CR, Park YW, Heeger AJ, Shirakawa H, Louis EJ, Gau SC, MacDiarmid AG (1977) Phys Rev Lett 39:1098
6. Chiang CK, Druy MA, Gau SC, Heeger AJ, Louis EJ, MacDiarmid AG, Park YW, Shirakawa H (1978) J Am Chem Soc 100:1013
7. Smie A, Heinze J (1997) Angew Chem 109:375
8. Mizes HA, Conwell EM (1993) Phys Rev Lett 70:1505
9. Zuppiroli L, Bussac MN, Paschen S, Chauvet O, Forro L (1994) Phys Rev B 50:5196
10. Damlin P, Kvarnström C, Ivaska A (1999) Electrochim Acta 44:4087
11. Petr A, Dunsch L, Neudeck A (1996) J Electroanal Chem 412:153
12. Tian B, Zerbi G, Schenk R, Mullen K (1991) J Chem Phys 95:3191
13. Lefrant S, Perrin E, Buisson JP, Eckhardt H, Han CC (1989) Synth Met 29:E91
14. Sakamoto A, Furukawa Y, Tasumi M (1992) J Phys Chem 96:1490
15. Lefrant S, Buisson JP, Eckardt H (1990) Synth Met 37:91
16. Wery J, Dulieu B, Bullot J, Baitoul M, Deniard P, Buisson JP (1999) Polymer 40:519
17. Nguyen TP, Tran VH, Destruel P, Oelkrug D (1999) Synth Met 101:633
18. Mulazzi E, Ripamonti A, Wery J, Dulieu B, Lefrant S (1999) Phys Rev B 60:16519
19. Zerbi G, Galbiati E, Gallazzi MC, Castiglioni C, Del Zoppo M, Schenk R, Mullen K (1996) J Chem Phys 105:2509
20. Wery J, Dulieu B, Launay E, Bullot J, Baitoul M, Buisson JP (1997) Synth Met 84:277
21. Orion I, Buisson JP, Lefrant S (1998) Phys Rev B 57:7050
22. Damlin P, Kvarnström C, Ivaska A (1999) Anal Chim Acta 385:175
23. Damlin P, Kvarnström C, Ivaska A (2001) Synth Met 123:141
24. Schrader B (1989) Raman/infrared atlas of organic compounds, 2nd edn. VCH, Weinheim
25. Woo HS, Lhost O, Graham SC, Bradley DDC, Friend RH, Quattrocchi C, Bredas JL, Schenk R, Mullen K (1993) Synth Met 59:13
26. Tian B, Zerbi G, Schenk R, Mullen K (1991) J Chem Phys 95:3191

27. Sakamoto A, Furukawa Y, Tasumi M (1994) J Phys Chem 98:4635
28. Baitoul M, Wery J, Buisson JP, Arbuckle G, Shah H, Lefrant S, Hamdoume M (2000) Polymer 41:6955
29. Heinze J (2001) In: Lund H, Hammerich O (eds) Organic electrochemistry, 4th edn. Dekker, New York, p 1309
30. Sakamoto A, Furukawa Y, Tasumi M (1992) J Phys Chem 96:3870
31. Baitoul M, Buisson JP, Lefrant S, Dulieu B, Wery J, Lapkowski M (1997) Synth Met 84:623
32. Lefrant S, Buisson JP, Baitoul M, Orion I (1996) Pure Appl Opt 5:613
33. Baitoul M, Wery J, Dulieu B, Lefrant S, Buisson JP, Hamdoune M (1999) Synth Met 101:173
34. Sakamoto A, Furukawa Y, Tasumi M (1997) J Phys Chem B 101:1726
35. Furukawa Y, Ohtsuka H, Tasumi M (1993) Synth Met 55: 516
36. Tian B, Zerbi G, Mullen K (1991) J Chem Phys 95:8
37. Tian B, Zerbi G (1991) Synth Met 41–43:255
38. Bredas JL, Chance RR, Silbey R (1982) Phys Rev B 26:5843
39. Bredas JL, Themans B, Fripiat JG, Andre JM, Chance RR (1984) Phys Rev B 29:6761
40. Shimoi Y, Abe S (1994) Phys Rev B 50:14781